ACS APPLIED MATERIALS & INTERFACES

Research Article

www.acsami.org

# Suppressing Bacterial Interaction with Copper Surfaces through Graphene and Hexagonal-Boron Nitride Coatings

Carolina Parra,*[,†] Francisco Montero-Silva,[‡] Ricardo Henríquez,[†] Marcos Flores,[§] Carolina Garín,[†] Cristian Ramírez,[∥] Macarena Moreno,[†] Jonathan Correa,[†,⊥] Michael Seeger,[‡] and Patricio Häberle[†]

[†]Departamento de Física, Universidad Técnica Federico Santa María, Avenida España 1680, Valparaíso, Chile

[‡]Departamento de Química, Universidad Técnica Federico Santa María, Avenida España 1680, Valparaíso, Chile

[§]Departamento de Física, Facultad de Ciencias Físicas y Matemáticas, Universidad de Chile, Avenida Blanco Encalada 2008, Santiago, Chile

[∥]Departamento de Ingeniería Química y Ambiental, Universidad Técnica Federico Santa María, Avenida España 1680, Valparaíso, Chile

[⊥]Instituto de Física, Pontificia Universidad Católica de Valparaíso, Avenida Universidad 330, Curauma, Valparaíso, Chile

Supporting Information

**ABSTRACT:** Understanding biological interaction with graphene and hexagonal-boron nitride (h-BN) membranes has become essential for the incorporation of these unique materials in contact with living organisms. Previous reports show contradictions regarding the bacterial interaction with graphene sheets on metals. Here, we present a comprehensive study of the interaction of bacteria with copper substrates coated with single-layer graphene and h-BN. Our results demonstrate that such graphitic coatings substantially suppress interaction between bacteria and underlying Cu substrates, acting as an effective barrier to prevent physical contact. Bacteria do not "feel" the strong antibacterial effect of Cu, and the substrate does not suffer biocorrosion due to bacteria contact. Effectiveness of these systems as barriers can be understood in terms of graphene and h-BN impermeability to transfer $Cu^{2+}$ ions, even when graphene and h-BN domain boundary defects are present. Our results seem to indicate that as-grown graphene and h-BN films could successfully protect metals, preventing their corrosion in biological and medical applications.

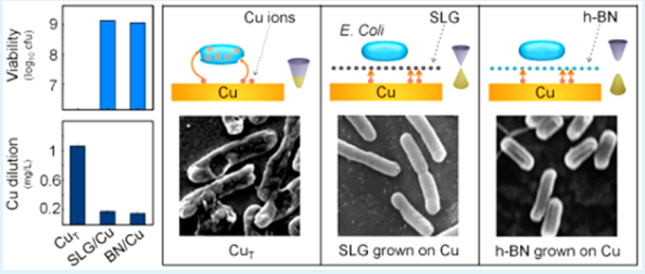


**KEYWORDS:** *graphene coating, biocorrosion, hexagonal boron nitride coating, copper, graphene impermeability*

## 1. INTRODUCTION

Potential applications of graphene, the unique two-dimensional (2D) allotrope of carbon, include electronic devices, sensors, photovoltaics, transistors, biotechnology, and desalination, among others. The incorporation of such technologies in consumer and industrial products is expected to have a significant impact on our daily lives. Whereas graphene is getting closer to mass production, reaching a complete understanding of its interaction with biological systems, such as bacteria and cells, is indeed a priority while considering expanding its uses in close contact with live organisms and allow further applications in biomedical products.

Bacterial interaction with surfaces is ubiquitous in nature. For centuries, human civilizations have used metallic copper in medicine, due to its antibacterial properties, until the advent of commercially available antibiotics in 1932. The most popular form of large-area graphene is, in fact, the one grown on copper due to high quality−cost ratio. Graphene-coated copper foils have been reported to serve as an ultrathin physical barrier, preventing direct interaction between underlying metal and ambient oxygen.[1−3] This anticorrosion property has been recently confirmed to be a short-term effect of graphene coating which, in the end, causes the room-temperature long-term oxidation of copper.[4] However, when bacterial interaction with a material is studied, short-term interactions become relevant. The U.S. Environmental Protection Agency (EPA), for example, defines a material as antimicrobial if it kills 99.9% of most bacteria within 2 h.[5] Another example of bacterial interaction is biocorrosion, which is a type of metal corrosion that occurs when microorganisms present in different environments alter metal−solution interface condition causing a strong interaction that considerably accelerates mechanical failure of metals in a wide range of environments.[6,7] This type of corrosion induced by microorganisms is a major issue in sectors such as metallurgy and construction, which have reported costs of hundreds of millions of dollars in maintenance and repairing damaged infrastructures.[8−10]

Received: September 8, 2014
Accepted: March 16, 2015
Published: March 16, 2015





DOI: 10.1021/acsami.5b01248
ACS Appl. Mater. Interfaces 2015, 7, 6430−6437

There are many reports of bacterial interaction with graphene oxide (GO) formed by micro- or nanosized flakes of functionalized graphene in powder or solution,[11,12] which emphasize rupture of the cell membrane as its antibacterial mechanism. Flake size turns out to be a relevant aspect for the reported antibacterial activity of GO.[13] However, in the case of single-layer graphene (SLG) sheets grown on Cu, which are 1 atom thick as GO, they have surface areas in the square centimeter range. Hence, the mechanism of the bacterial interaction must be different in both cases, and in fact, recent studies have shown contradictory results regarding in this regard. Inductively coupled plasma (ICP) measurements have shown that graphene greatly reduces the available $Cu^{2+}$ ion[14] which, according to the most accepted theory for the bacteria killing mechanism of copper,[15] are responsible of copper antibacterial activity. Reports of graphene being chemically inert and impermeable support this claim.[16−18] In contract, electron transfer from microbial membranes to graphene has been reported to produce a strong antibacterial effect in this system.[19]

Motivated by this contradiction, in this report, we present a complete study on the interaction of bacteria with graphene- and hexagonal-boron nitride-coated copper surfaces. We focus on how such graphitic membranes modify (1) the antibacterial effect of Cu (the way microorganisms "feel" Cu surfaces) and (2) the Cu biocorrosion process (the way Cu "feels" bacteria). For the first scenario, antibacterial activity of Cu foils coated with SLG and single layer hexagonal-boron nitride (h-BN) was evaluated and compared to metallic substrates without such graphitic coatings. For the second scenario, biocorrosion of coated and uncoated Cu foils in contact to bacteria were studied. Single-layer h-BN was chosen due to its graphene-type atomic structure and wide electronic band gap both within and across the layer.[20,21] This is indeed in contrast to SLG, which displays a high electrical conductivity.[22] Such differences could help elucidate any connection between electronic properties and antibacterial activity of graphitic-like membranes. In addition, graphene transferred onto Cu surfaces was included in this study to establish a comparison between antibacterial performances of these coatings obtained through different methodologies.

Our observations demonstrated that an as-grown graphene coating blocks both the antibacterial activity and biocorrosion of Cu surface, acting as an effective protective membrane that prevents contact between bacteria and metal. The same results were obtained for single layer h-BN grown on Cu. Intrinsic low-quality coating of transferred graphene on Cu foils leads to similar bacterial interaction of bare materials. For this study, antibacterial and biocorrosion properties of thermally treated Cu were analyzed. The fact that single-layer h-BN (insulating) is as effective as graphene (conducting) to prevent contact of bacteria with the underlying substrate emphasizes the lack of connection between charge transfer through these 2D membranes and their antibacterial activity, as was claimed in previous studies.[19]

## 2. EXPERIMENTAL SECTION

Commercial SLG grown on Cu foil and single-layer h-BN grown on Cu were used for this study. Samples of 1 $cm^2$ surface area were used for all measurements. Corresponding Cu control substrates (CuT) were prepared treating fresh Cu (CuF) foils (99.8%, Alfa Aesar, 20 $\mu$m thickness) under the same temperature and hydrogen pressure conditions used for graphene growth (Supporting Information) but without the carbon precursor gas. PMMA-assisted transfer method[23,24] was used in order to obtain transferred graphene on $SiO_2$ and CuF and CuT, samples (Figure S1, Supporting Information).

A combination of scanning electron microscopy (SEM) (Carl Zeiss, EVO MA-10), scanning tunneling microscopy (UHV-VT Omicron) and X-ray photoelectron spectrometry (XPS; PerkinElmer PHI 1257, Al K$\alpha$ source, 1486.6 eV) was used to characterize the morphology and chemical environment of all samples. MicroRaman measurements (Renishaw, 532 nm laser) were used to characterize quality of as-grown and transferred graphene and h-BN. Contact angle measurements were performed to characterize surface hydrophobicity of coated and uncoated Cu samples. A drop of Milli-Q water (2 $\mu$L) was placed on the surface of graphene- and h-BN-coated Cu samples, and images were immediately captured using a high-resolution camera. The contact angle was measured using the image processing software ImageJ.[25]

To explore the bacterial response of graphene coatings, we used *Escherichia coli* MG1655 cultures. Bacterial cultures were grown until prestationary growth phase in a low ionic strength medium that contained meat extract (5 g $L^{-1}$) and yeast extract (5 g $L^{-1}$). The bacterial cultures were concentrated by centrifugation (5000*g*, 5 min), washed three times with Milli-Q water, and finally resuspended up to a turbidity of 3.0 at 600 nm. The turbidity of this stock dispersion is equivalent to a bacterial concentration of $\sim 1 \times 10^9$ CFU $mL^{-1}$. Milli-Q water was used as dispersant to avoid bacterial duplication and the forthcoming accumulation of mineral crystals that may interfere with the collection of microscopy images or cause unwanted chemical reactions with the samples.

Cell viability (inverse to cell death) was monitored to evaluate the antibacterial activity of coated and uncoated Cu samples. One volume (100 $\mu$L) of *E. coli* MG1655 stock dispersion was placed on each sample surface in order to obtain a final bacterial density of 60 $\mu$L/$cm^2$. Sample+bacteria systems were incubated at 37 °C during 24 h in a humidity chamber to avoid evaporation. Once this incubation period was completed, bacteria were recovered with 3 volumes of Milli-Q water using a standard micropipette. Cell viability at 0 and 24 h was determined using the microdot methodology.[26] Each experimental trial was conducted in triplicate. For SEM characterization, bacteria were fixed on samples with 3% (v/v) glutaraldehyde and dehydrated by washing with a graded ethanol series (from 10 to 100%), followed by critical-point drying and gold coating.

Copper release from metallic surfaces was determined by atomic absorption spectroscopy (AAS) using a Spectraa-800 spectrophotometer Varian. Coated and uncoated Cu foils were exposed to bacterial cultures using the same experimental parameters previously described for viability measurements. Control samples (CuT) were exposed to Milli-Q water without bacteria. After 24 h, bacteria were recovered, poured into 2.5 mL of 15 $\mu$M EDTA solution (pH 10) and centrifuged at 5000*g* during 10 min. The supernatant was recovered, and the total Cu concentration was quantified by AAS.

## 3. RESULTS AND DISCUSSION

Micrometer scale morphological characterization of samples prior to bacterial contact was supplemented by SEM (Figure S2, Supporting Information). Fresh Cu samples (Figure S2a,b in the Supporting Information) show well-defined stripes across their surfaces. In contrast, thermally treated Cu foils (CuT; Figure S2c,d, Supporting Information) exhibited a smooth surface covered with deep grain boundaries (size ~15 $\mu$m), evidence of the irreversible damage to the foil's microstructure known as hydrogen embrittlement.[27] This process is caused by the high-temperature treatment of foils in a hydrogen atmosphere before graphene growth. We specifically included the influence of this phenomenon in the bacterial interaction by choosing graphene transferred on untreated Cu foils (CuF). Such systems allowed us the opportunity to explore the performance of graphitic membranes when transferred on undamaged foils, which is closer to more realistic applications.


DOI: 10.1021/acsami.5b01248
ACS Appl. Mater. Interfaces 2015, 7, 6430−6437

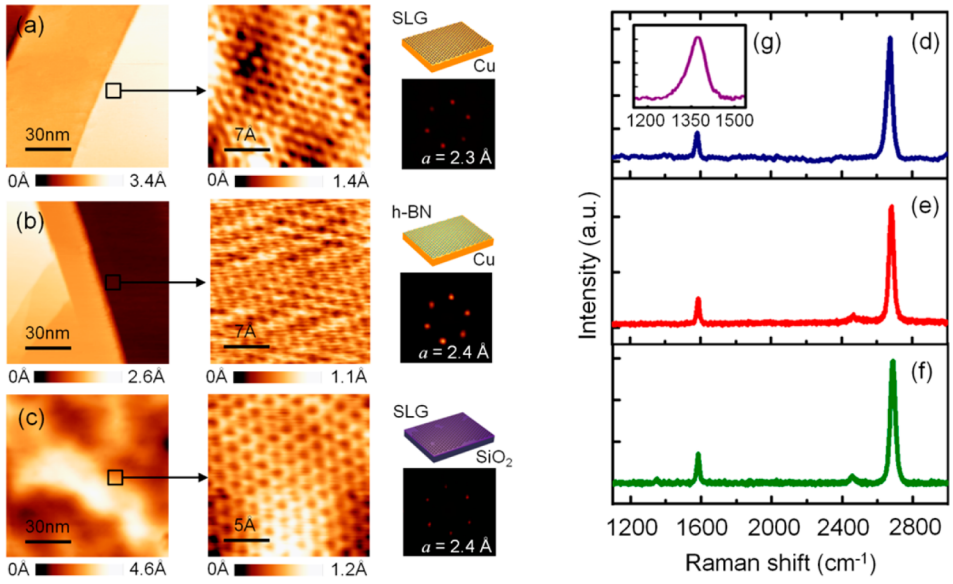


**Figure 1.** STM topographies of graphene- and h-BN-coated Cu samples: (a) Large-scale STM topographic image (100 × 100 nm) of SLG grown on Cu showing typical terrace topography ($I$ = 0.1 nA, $V_{BIAS}$ = −0.2 V). Atomically resolved image (2.5 × 2.5 nm) shows a near-hexagonal lattice of monolayer graphene (inset) with lattice distance 2.4 Å, according to 2-D Fourier transform analysis. (b) High bias STM image of h-BN grown on Cu samples ($I$ = 0.6 nA, $V_{BIAS}$ = 1.2 V) and the corresponding hexagonal lattice form by B−N atoms ($I$ = 0.6 nA, $V_{BIAS}$ = 1.2 V). (c) Graphene honeycomb lattice can be clearly resolved in the case of SLG transferred on $SiO_2$ ($I$ = 0.04 nA, $V_{BIAS}$= −0.15 V). Representative Raman spectra of (d) SLG grown on Cu, (e) SLG transferred on $SiO_2$, (f) SLG transferred on Cu and (g) Ssingle-layer h-BN grown on Cu and transferred to $SiO_2$. Background caused by the luminescence of the copper was subtracted in the case of SLG grown and transferred on Cu.

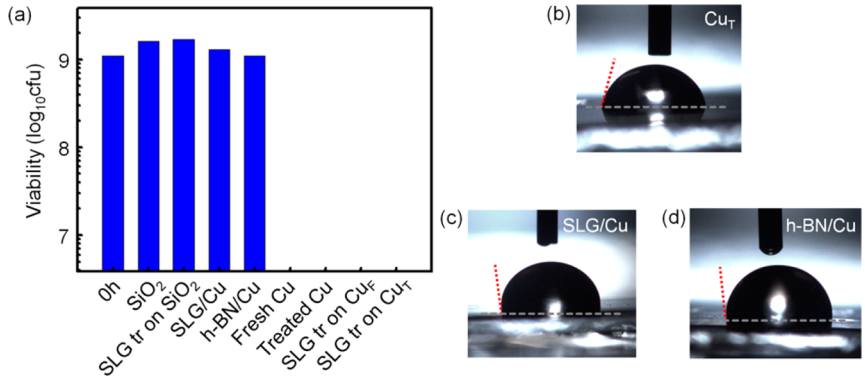


**Figure 2.** (a) Cell viability of *E. coli* MG1685 exposed to different samples after 24 h. Blue columns show results for SLG- and h-BN-coated Cu samples (and corresponding control, $SiO_2$ and SLG tr on $SiO_2$). Typical photographs of cultivated *E. coli* colonies on agar plates are shown in Figure S2 (Supporting Information). Images of contact angle measurements using Milli-Q water in contact with (b) CuT, (c) SLG grown on Cu, (d) and h-BN grown on Cu.

Scanning electron micrographs of SLG grown on Cu and h-BN grown on Cu showed some contrast that could be identified as graphene domains. However, as has been reported, there are serious difficulties in clearly distinguishing the graphitic material using this technique.[28] The surface of transferred SLG onto Cu foil showed micrometric damages in the graphitic membrane product of the transfer procedure, which leaves some Cu areas exposed (bright areas in Figure S2h, Supporting Information).

We have used scanning tunneling microscopy (STM) in ultrahigh vacuum conditions to visualize SLG grown on Cu, h-BN grown on Cu and SLG transferred to $SiO_2$ with nanoscale resolution. Characteristic fingerprints of high-quality graphitic materials[29,30] were observed through atomic-resolved topographies. A hexagonal structure with 2.3 Å lattice distance (according to Fourier transform analysis) was observed for SLG grown on Cu (Figure 1a), in agreement with expected values for this graphitic material.[30] A typical large-scale topography of h-BN (Figure 1b) shows h-BN-coated Cu terraces, revealing atomic resolved hexagonal lattice for high-resolution image (inset). The absence of electronic coupling to a metallic substrate, in the case of SLG transferred to $SiO_2$, allows a clearer visualization of the intrinsic hexagonal structure (honeycomb) of graphene (Figure 1c). A clean surface is a critical aspect for this type of probe microscopy images and, in the case of transferred graphene sheets, few signs of surface contamination were found.

To verify the graphitic quality of graphene and h-BN coatings, we performed microRaman measurements. Multiple areas of each sample were analyzed, and representative spectra are shown in Figure 1. Our SLG on Cu samples (SLG grown on Cu, Figure 1d; SLG transferred on $SiO_2$, Figure 1f; and SLG transferred on Cu, Figure 1g) typically display sharp G (1584 $cm^{-1}$) and 2D (2680−2693 $cm^{-1}$) bands, with a small G/2D


DOI: 10.1021/acsami.5b01248
ACS Appl. Mater. Interfaces 2015, 7, 6430−6437

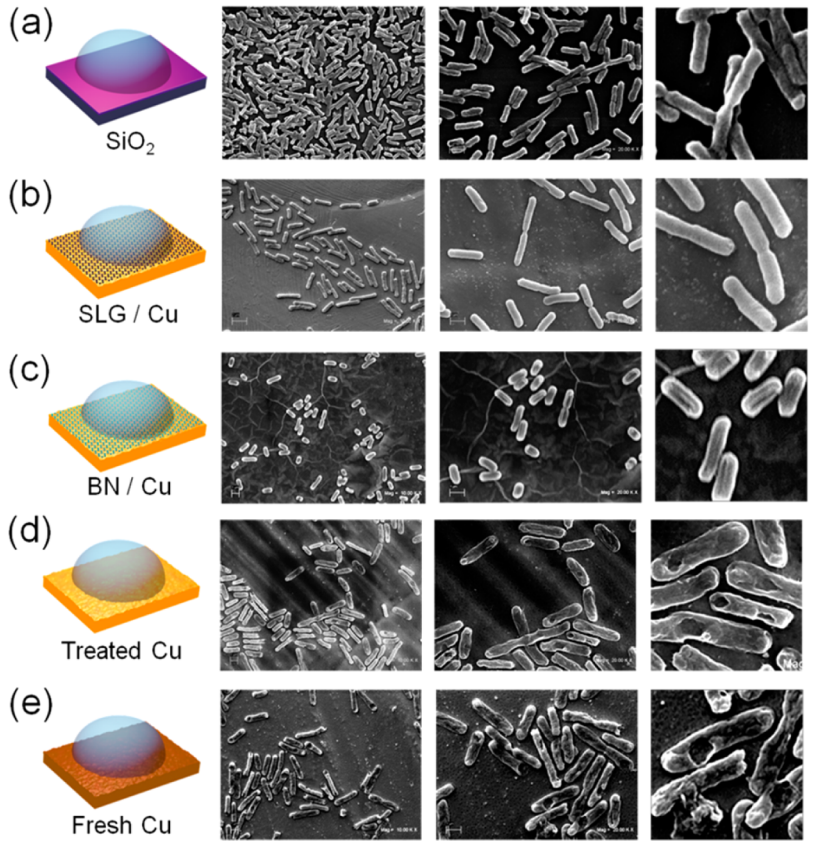


**Figure 3.** SEM images of *E. coli* after 24 h of incubation on different samples (scale bars correspond to 1 $\mu$m in all cases except in the left panel, where it corresponds to 2 $\mu$m). (a) $SiO_2$, (b) SLG grown on Cu, (c) single-layer h-BN grown on Cu, (d) treated Cu (CuT), and (e) fresh Cu (CuF). After 1 day of incubation on CuT and CuF, bacteria exhibit highly damaged membranes, irregular shapes, and rough surfaces, a clear sign of cell lysis. Similar damage was found in bacteria incubated on graphene transferred on CuF and CuT samples (Figure S5b,c, Supporting Information). In contrast, intact and smooth bacteria surface were observed when incubated on graphene- and h-BN-coated Cu foils, indicating such coatings substantially decrease the toxicity of the Cu substrate to bacteria.

ratio (0.25, 0.29, and 0.28 respectively). These results are consistent with SLG, according to values reported in literature.[31−33] In our single-layer h-BN grown on Cu sample (Figure 1h), the Raman peak occurs at ∼1369 $cm^{-1}$ but with intensity ∼5 times smaller than that for graphene's G peak under the same measurement conditions.

Figure 2 summarizes cell viability results on *E. coli* after 24 h of incubation on graphene-coated Cu samples, h-BN-coated Cu and control. Cell viability percentage (viability%) was calculated comparing CFU at 24 h and at $t = 0$ (Figure S3, Supporting Information). After 1 day of incubation, both h-BN and SLG grown on Cu samples show a viability% of 100 and 118%, respectively. This indicates no interaction between Cu ions and bacteria after 24 h. In contrast, cell viability for CuF and CuT was zero, in agreement with the expected contact killing of bacteria on Cu.[34]

Antibacterial effect for CuT and CuF was monitored at 2 h to quantify their differences as a function of time (Figure S4, Supporting Information). The corresponding antibacterial efficiencies (100% viability%) after 2 h for CuF was 30%, whereas 87% was obtained for CuT, indicating a higher bactericidal activity for treated Cu. The same antimicrobial efficiency of bare Cu at 24 h (100%) was obtained for transferred graphene on Cu foil, which is probably connected to the intrinsic defects of graphene coatings on these samples (Figure S2h, Supporting Information).

When bacterial interaction with surfaces is studied, bacterial adhesion need to be considered as a relevant parameter. Upon approach of a surface, microorganisms will be attracted or repelled, depending on the resultant of the different nonspecific interaction forces.[35] Among these, hydrophobic force is one of the most important properties involved in the adhesion process and is determined by physicochemical surface properties.[36] Bacteria are more prone to attach to the hydrophobic surfaces rather than hydrophilic[37] surfaces, and hydrophobicity of the cell surface, like the reported for *E. coli*,[37] tends to increase adhesion.[38]

Contact angle measurements were performed using 2 $\mu$L of Milli-Q water on graphene-coated and uncoated Cu to determine the influence of possible hydrophobic characteristics of metallic substrate surfaces over bacterial adhesion process and, in consequence, over bacterial interaction with such surfaces. In the case of copper, there is a clear transition from hydrophilic surface (contact angle of ∼82°) for treated copper substrate (Figure 2b) to a hydrophobic surface when copper is covered by graphitic membranes, such as SLG and h-BN (contact angle of ∼98° and ∼103°, Figure 2c,d). Our contact angle measurements show that, considering bacterial adhesion is promoted from a physicochemical point of view by hydrophobic metal and cell surface, graphitic coatings are expected to increase physical contact between bacteria and coated Cu surface.



DOI: 10.1021/acsami.5b01248
*ACS Appl. Mater. Interfaces* 2015, 7, 6430−6437

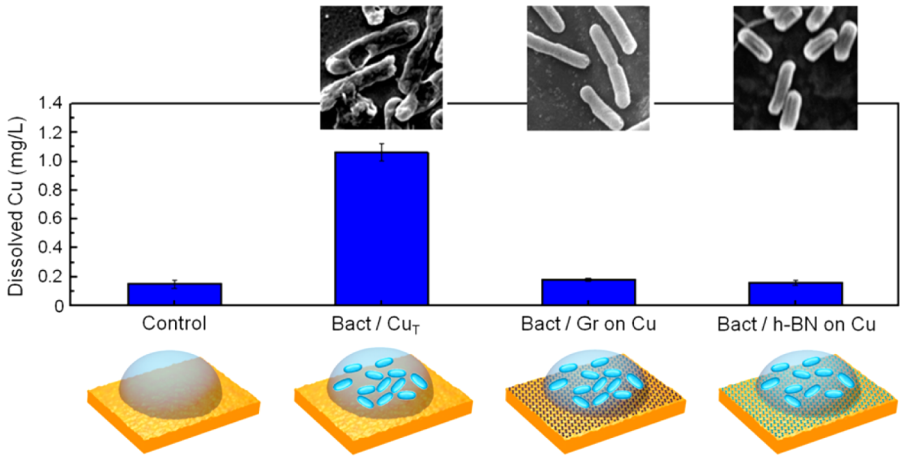


**Figure 4.** AAS measurements on coated and uncoated Cu samples after 24 h of bacteria contact showing Cu dissolution. Dissolved Cu for h-BN- and graphene-coated Cu samples in contact to bacteria is below the detection limit, as well as control sample. Only bare CuT in contact with bacteria present Cu dissolution.

Morphology of bacteria incubated on control samples and on graphene- and h-BN-coated Cu samples is shown in Figure 3. A smooth cell surface is observed for bacteria on control $SiO_2$ (Figure 3a). The same intact bacteria surface with regular shape is seen in the case of *E. coli* on SLG grown on Cu (Figure 3b) and single-layer h-BN grown on Cu (Figure 3c), in agreement with our viability results. Cu-exposed bacteria (Figure 3d,e) exhibit a wide range of significant abnormalities, such as the collapse of the cell structure and a ghost-like appearance in which bacteria seem transparent, looking empty and flat. Such morphological features in bacterial cells are due to the lysis of the outer membrane followed by the loss of cellular electron-dense materials, a well-defined pattern for bacteria cell damaged on copper surfaces.[39,40] Similarly, irregular shapes, damaged membranes, and rough surfaces were found in bacteria in contact with graphene transferred on CuF and CuT samples for 24 h (Figure S5b,c, Supporting Information) compared to SLG transferred on $SiO_2$ (Figure S5a, Supporting Information), which acts as control sample for transferred membranes.

Dissolution of copper was studied by AAS to quantify biocorrosion of coated and uncoated Cu samples due to contact with bacterial cultures. Figure 4 shows the concentration of Cu release from Cu samples exposed to bacteria for 24 h. CuT in contact to Milli-Q water without *E. coli* cells was chosen as control sample. Dissolved Cu for h-BN- and graphene-coated Cu samples in contact to Milli-Q water with bacteria is below the detection limit of the technique, as well as control sample. Only bare CuT in contact with bacteria presents an evident metal dissolution. These results demonstrate graphitic two-dimensional membranes efficiently protect underlying Cu from biocorrosion due to bacterial interaction. In particular, Cu dissolution is found to be inversely related to cell viability (Figure 2), which is in agreement with the proposed mechanism of Cu toxicity, which is thought to be influenced mostly by the influx of copper ions into the cells.

The observed effectiveness of graphene and h-BN as a barrier against bacteria and underlying Cu interaction can be understood in terms of graphene permeability. Graphene's p-orbitals form a dense and delocalized cloud that blocks the gap within its aromatic rings,[41] creating a repelling field that does not allow molecules to pass through. The reported graphene pore size is 64 pm,[20] a value smaller than the effective ionic radii of $Cu^{2+}$ (73 pm) and $Cu^{1+}$ (77 pm), which are responsible for the antibacterial properties of Cu.[15] According to our results, even defects at graphene domain boundaries[42,43] (inherent of CVD growth method) are efficiently preventing the passage of Cu ions through the graphitic membrane as well. Additionally, graphene and hexagonal BN have very similar lattice constant (h-BN in-plane lattice constant of 2.5 A is only mismatched to graphene by 1.3%) and comparable van der Waals radius,[43,44] which, in the same way, can explain the observed impermeability of BN membranes to Cu ions transfer (see Figure 6d for illustrative diagram). If we consider an increased attachment (adhesion) of *E. coli* to coated Cu surface samples due to hydrophobic interaction, then the proposed protection mechanism of such impermeable graphitic coatings is proven to be efficient even under more critical conditions.

XPS analysis was performed to provide surface composition information that can be connected to the bacterial response of the different substrates (Figure 5). In particular, we focused on

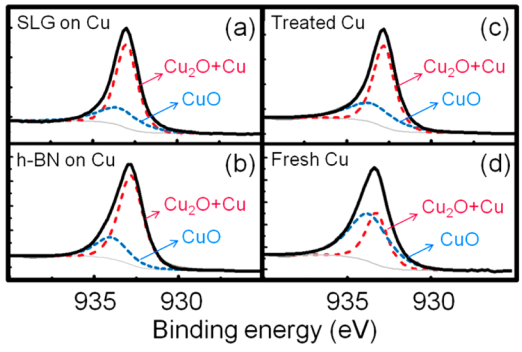


**Figure 5.** XPS Cu $2p_{3/2}$ spectra of coated and uncoated Cu foils, including peak fitting to identify Cu, $Cu_2O$, and CuO contributions. (a) SLG grown on Cu, (b) single-layer h-BN grown on Cu, (c) treated Cu, and (d) fresh Cu.

the Cu $2p_{3/2}$ peak, which contains information on Cu, CuO, and $Cu_2O$ surface contents.[45] $Cu_2O$ and Cu signals were regarded as one peak, considering that the XPS bands that originated from them are virtually identical.[46] Corresponding CuO and $Cu_2O$+Cu peaks for SLG grown on Cu (932.9 and 933.4 eV), h-BN grown on Cu (932.8 and 933.9 eV) and CuT (932.8 and 933.5 eV) show similar features in terms of positions and intensities. The corresponding contents of $Cu_2O$


DOI: 10.1021/acsami.5b01248
ACS Appl. Mater. Interfaces 2015, 7, 6430−6437

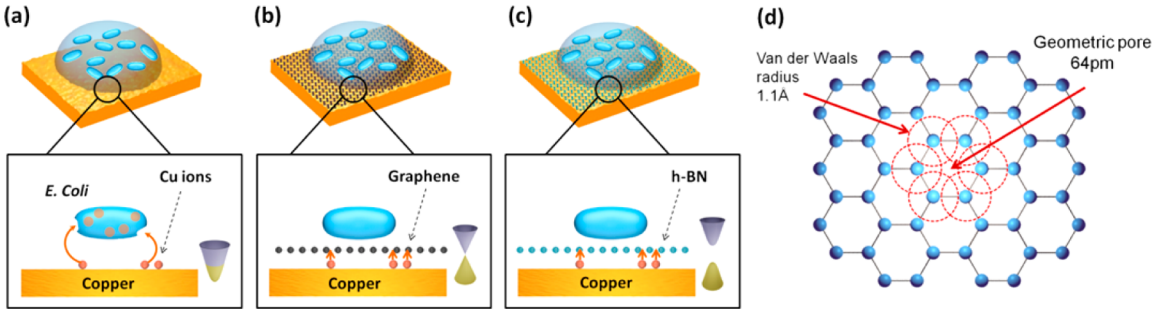


**Figure 6.** Schematic illustration of bacteria-coated copper interaction inferred from our study. (a) Bare Cu (fresh or treated) exhibits antibacterial activity producing membrane damage, copper influx into the cells, oxidative damage, and cell death. (b) For graphene-coated Cu, there is no interaction between bacteria and underlying substrate, leading to inhibition of Cu antibacterial activity due to this highly conductive nanoscale coating. In addition, absence of biocorrosion of Cu is observed. (c) In the case of h-BN-coated Cu, the same lack of interaction between metal and bacteria is observed, even when considering insulating properties of such coating. (d) Pore size of graphene (similar to corresponding for h-BN) determines impermeability to Cu ions, which are responsible of its antibacterial activity. Both graphitic coatings suppress interaction between bacteria and metal, protecting bacteria from antibacterial properties of Cu and Cu from biocorrosion due to bacteria contact.

+Cu were 71.6% for SLG grown on Cu, 75.6% for h-BN grown on Cu, and 65.4% for CuT, indicating a strong metallic signal for all these samples.

Such a result is expected, considering the oxide removal thermal treatment to which the samples were subjected prior to graphene growth. Additionally, this measurement clearly indicates that CuT and not CuF is, in fact, the "real control sample" of graphene-coated Cu foils for antibacterial studies due to the similarity of Cu+$Cu_2O$ content in both samples. On the other hand, CuF has a stronger CuO signal (62.9%), an oxide species with lower bactericide activity.[5] This result is in agreement with the diminished 51.3% antibacterial efficiency observed after 2 h for this sample (Figure S4, Supporting Information).

Figure 6 summarizes the interaction between bacteria and graphene- and h-BN-coated Cu substrates, inferred from our study. Figure 6a shows the typical "contact killing" phenomenon observed in the case of Cu substrate (fresh or treated) which proceeds by successive membrane damage, copper influx into the cells, oxidative damage and cell death. Our AAS measurements are in agreement with this antibacterial mechanism. When metallic substrate is covered by an as-grown graphitic membrane, regardless of its electrical properties, we observed inhibition of all Cu antibacterial activity and Cu biocorrosion, leading to (1) intact bacteria, as our viability measurements and SEM micrographs have confirmed, and (2) absence of Cu dissolution, as our AAS measurements have shown. Such behavior indicates that there is no physical or electrical interaction between underlying Cu and bacteria (Figure 6b,c). This effect is presumably connected to impermeability of graphene and h-BN membranes to Cu ions transfer (Figure 6d).

## 4. CONCLUSION

In conclusion, we studied the interaction between bacteria and graphene- and h-BN-coated Cu samples. Our findings clearly show both graphene and h-BN coating substantially suppress interaction between bacteria and underlying Cu substrate. From the bacteria perspective, metal toxicity (connected to Cu ions influx into cells) is suppressed and with regard to the effect on the Cu substrate, biocorrosion, due to bacteria in contact to metal surface, is prevented. The fact that both a conducting (graphene) and an insulating (h-BN) membrane, with almost the same lattice constant, equally suppressed antibacterial properties of Cu suggests that a connection between charge transfer from metal to bacteria through these 2D systems and their antimicrobial activity is less likely. On the other hand, impermeability of the graphene and h-BN membranes is strong enough to prevent all exchange of Cu ions through it, even considering typical grain boundary defects and the hydrophobic properties of cells and coatings. At the end, this effect determines the lack of antibacterial activity and the consequent absence of biocorrosion of coated Cu foils. Our results indicate as-grown graphene and h-BN films could successfully protect metals and prevent their corrosion in biological environments linked to medical applications.

## ■ ASSOCIATED CONTENT

### Supporting Information

Detailed description of PMMA-assisted graphene transfer method and Cu foils thermal treatment; morphological characterization of samples prior to bacterial contact; typical photographs of cultivated *E. coli* on agar plates for different substrates; 2 h viability results for fresh and treated copper; SEM images of *E. coli* after 24 h incubation on SLG transferred on $SiO_2$, SLG transferred on CuF, and SLG transferred on CuT. This material is available free of charge via the Internet at http://pubs.acs.org.

## ■ AUTHOR INFORMATION

### Corresponding Author

*E-mail: carolina.parra@usm.cl.

### Notes

The authors declare no competing financial interest.

## ■ ACKNOWLEDGMENTS

This work was financially supported by Conicyt de Inserción nos. 791220009 and 791100037, Fondecyt grant nos. 1110935 and 1110992, Proyecto Interno DGIP nos. 111469 and 111470, PIA anillo ACT 1117. FMS gratefully acknowledges the support of CONICYT Ph.D., Mecesup FSM1204, and UTFSM-PIIC fellowships.

## ■ REFERENCES

(1) Chen, S. S.; Brown, L.; Levendorf, M.; Cai, W. W.; Ju, S. Y.; Edgeworth, J.; Li, X. S.; Magnuson, C. W.; Velamakanni, A.; Piner, R. D.; et al. Oxidation Resistance of Graphene-Coated Cu and Cu/Ni Alloy. *ACS Nano* **2011**, *5*, 1321−1327.



DOI: 10.1021/acsami.5b01248
*ACS Appl. Mater. Interfaces* 2015, 7, 6430−6437

(2) Nilsson, L.; Andersen, M.; Balog, R.; Laegsgaard, E.; Hofmann, P.; Besenbacher, F.; Hammer, B.; Stensgaard, I.; Hornekaer, L. Graphene Coatings: Probing the Limits of the One Atom Thick Protection Layer. *ACS Nano* **2012**, *6*, 10258−10266.
(3) Topsakal, M.; Sahin, H.; Ciraci, S. Graphene Coatings: An Efficient Protection from Oxidation. *Phys. Rev. B* **2012**, *85*, 155445−155451.
(4) Zhou, F.; Li, Z.; Shenoy, G. J.; Liand, L.; Liu, H. Enhanced Room-Temperature Corrosion of Copper in the Presence of Graphene. *ACS Nano* **2013**, *7*, 6939−6947.
(5) Hans, M.; Erbe, A.; Mathews, S.; Chen, Y.; Solioz, M.; Mücklich, F. Role of Copper Oxides in Contact Killing of Bacteria. *Langmuir* **2013**, *29*, 16160−16166.
(6) Rao, T. Microbial Fouling and Corrosion: Fundamentals and Mechanisms. In *Operational and Environmental Consequences of Large Industrial Cooling Water Systems*; Rajagopal, S., et al., Eds.; Springer: New York, 2012; pp 95−126.
(7) Stoodley, P.; Sauer, K.; Davies, D. G.; Costerton, J. W. Biofilms as Complex Differentiated Communities. *Annu. Rev. Microbiol.* **2002**, *56*, 187−209.
(8) Li, K.; Whitfield, M.; Van Vliet, K. J. Beating the Bugs: Roles of Microbial Biofilms in Corrosion. *Corros. Rev.* **2013**, *31*, 73−84.
(9) Sreekumari, K. R.; Sato, Y.; Kikuchi, Y. Antibacterial Metals. A Viable Solution for Bacterial Attachment and Microbiologically Influenced Corrosion. *Mater. Trans.* **2005**, *46*, 1636−1645.
(10) Keevil, C. W. The Physico-Chemistry of Biofilm-Mediated Pitting Corrosion of Copper Pipe Supplying Potable Water. *Water Sci. Technol.* **2010**, *49*, 91−98.
(11) Yu, L.; Zhang, Y.; Zhang, B.; Liu, J.; Zhang, H.; Song, C. Preparation and Characterization of HPEI-GO/PES Ultrafiltration Membrane with Antifouling and Antibacterial Properties. *J. Membr. Sci.* **2013**, *447*, 452−462.
(12) Yu, L.; Zhang, Y.; Zhang, B.; Liu, J. Enhanced Antibacterial Activity of Silver Nanoparticles/Halloysite Nanotubes/Graphene Nanocomposites with Sandwich-Like Structure. *Sci. Rep.* **2014**, *4*, 4551−4555.
(13) Al-Thani, R. F.; Patan, N. K.; Al-Maadeed, M. A. Graphene Oxide as Antimicrobial Against Two Gram-positive and Two Gram-Negative Bacteria in Addition to One Fungus, OnLine. *J. Biol. Sci.* **2014**, *14*, 230−239.
(14) Zhang, W.; Lee, S.; McNear, K. L.; Chung, T. F.; Lee, S.; Lee, K.; Crist, S. A.; Ratliff, T. L.; Zhong, Z.; Chen, Y. P.; Yang, C. Use of Graphene as Protection Film in Biological Environments. *Sci. Rep.* **2014**, *4*, 4097−4105.
(15) Grass, G.; Rensing, C.; Solioz, M. Metallic Copper as an Antimicrobial Surface. *Appl. Environ. Microbiol.* **2011**, *77*, 1541−1547.
(16) Bunch, J. S.; Verbridge, S. S.; Alden, J. S.; van der Zande, A. M.; Parpia, J. M.; Craighead, H. G.; McEuen, P. L. Impermeable Atomic Membranes from Graphene Sheets. *Nano Lett.* **2008**, *8*, 2458−2462.
(17) Cho, J.; Gao, L.; Tian, J.; Cao, H.; Wu, W.; Yu, Q.; Yitamben, E. N.; Fisher, B.; Guest, J. R.; Chen, Y. P.; Guisinger, N. P. Atomic-Scale Investigation of Graphene Grown on Cu Foil and the Effects of Thermal Annealing. *ACS Nano* **2011**, *5*, 3607−3613.
(18) Lee, K. H.; Shin, H. J.; Lee, J.; Lee, I.; Kim, G.; Choi, J.; Kim, S. Large-Scale Synthesis of High-Quality Hexagonal Boron Nitride Nanosheets for Large-Area Graphene Electronics. *Nano Lett.* **2012**, *12*, 714−718.
(19) Li, J.; Wang, G.; Zhu, H.; Zhang, M.; Zheng, X.; Di, Z.; Liu, X.; Wang, X. Antibacterial Activity of Large-Area Monolayer Graphene Film Manipulated by Charge Transfer. *Sci. Rep.* **2014**, *4*, 4359−4366.
(20) Berry, V. Impermeability of Graphene and its Applications. *Carbon* **2013**, *62*, 1−10.
(21) Wu, J.; Wang, B.; Wei, Y.; Yang, R.; Dresselhaus, M. Mechanics and Mechanically Tunable Band Gap in Single-Layer Hexagonal Boron-Nitride. *Mater. Res. Lett.* **2013**, *1*, 200−206.
(22) Geim, A. K. Graphene: Status and Prospects. *Science* **2009**, *324*, 1530−1534.
(23) Reina, A.; Son, H.; Jiao, L.; Fan, B.; Dresselhaus, M. S.; Liu, Z.; Kong, J. Transferring and Identification of Single- and Few-Layer Graphene on Arbitrary Substrates. *J. Phys. Chem. C* **2008**, *112*, 17741−17744.
(24) Jia, C.; Jiang, J.; Gan, L.; Guo, X. Direct Optical Characterization of Graphene Growth and Domains on Growth Substrates. *Sci. Rep.* **2012**, *2*, 707−712.
(25) Stalder, A. F.; Kulik, G.; Sage, D.; Barbieri, L.; Hoffmann, P. A Snake-Based Approach to Accurate Determination of Both Contact Points and Contact Angles. *Colloids Surf.* **2006**, *286*, 92−103.
(26) Chirino, B.; Strahsburger, E.; Agulló, L.; González, M.; Seeger, M. Genomic and Functional Analyses of the 2-Aminophenol Catabolic Pathway and Partial Conversion of Its Substrate into Picolinic Acid in Burkholderia Xenovorans LB400. *PloS One* **2013**, *8* (10), e75746.
(27) Shin, Y. C.; Kong, J. Hydrogen-Excluded Graphene Synthesis Via Atmospheric Pressure Chemical Vapor Deposition. *Carbon* **2013**, *59*, 439−447.
(28) Kirkland, N. T.; Schiller, T.; Medhekar, N.; Birbilis, N. Exploring Graphene as a Corrosion Protection Barrier. *Corros. Sci.* **2012**, *56*, 1−4.
(29) Park, J.; Lee, J.; Liu, L.; Clark, K. W.; Durand, C.; Park, C.; Sumpter, B. G.; Baddorf, A. P.; Mohsin, A.; Yoon, M.; Gu, G.; Li, A. P. Spatially Resolved One-dimensional Boundary States in Graphene−Hexagonal Boron Nitride Planar Heterostructures. *Nat. Commun.* **2014**, *5*, 5403.
(30) Yu, Q.; Jauregui, L. A.; Wu, W.; Colby, R.; Tian, J.; Su, Z.; Cao, H.; Liu, Z.; Pandey, D.; Wei, D.; Chung, T. F.; Peng, P.; Guisinger, N. P.; Stach, E. A.; Bao, J.; Pei, S. S.; Chen, Y. P. Control and Characterization of Individual Grains and Grain Boundaries in Graphene Grown by Chemical Vapour Deposition. *Nat. Mater.* **2011**, *10*, 443−449.
(31) Li, X.; Cai, W.; An, J.; Kim, S.; Nah, J.; Yang, D.; Piner, R.; Velamakanni, A.; Jung, I.; Tutuc, E.; Banerjee, S. K.; Colombo, L.; Ruoff, R. S. Large-Area Synthesis of High-Quality and Uniform Graphene Films on Copper Foils. *Science* **2009**, *324*, 1312−1314.
(32) Ferrari, A. C.; Meyer, J. C.; Scardaci, V.; Casiraghi, C.; Lazzeri, M.; Mauri, F.; Piscanec, S.; Jiang, D.; Novoselov, K. S.; Roth, S.; Geim, A. K. Raman Spectrum of Graphene and Graphene Layers. *Phys. Rev. Lett.* **2006**, *97*, 187401−187405.
(33) Reina, A.; Jia, X.; Ho, J.; Nezich, D.; Son, H.; Bulovic, V.; Dresselhaus, M. S.; Kong, J. Large Area, Few-Layer Graphene Films on Arbitrary Substrates by Chemical Vapor Deposition. *Nano Lett.* **2008**, *9*, 30−35.
(34) Espirito Santo, D.; Elowsky, C. G.; Quaranta, D.; Domaille, D. W.; Chang, C. J.; Grass, G. Bacterial Killing by Dry Metallic Copper Surfaces. *Appl. Environ. Microbiol.* **2011**, *77*, 794−802.
(35) Gottenbos, B.; Busscher, H. J.; Van Der Mei, H. C.; Nieuwenhuis, P. Pathogenesis and Prevention of Biomaterial Centered Infections. *J. Mater. Sci.: Mater. Med.* **2002**, *13*, 717−722.
(36) Busscher, H. Specific and Non-specific Interactions in Bacterial Adhesion to Solid Substrata. *FEMS Microbiol. Lett.* **1987**, *46*, 165−173.
(37) Méndez-Vilas, A. *Microbial Pathogens and Strategies for Combating Them: Science, Technology and Education*; Formatex Research Center: Badajoz, Spain, 2013.
(38) Donlan, R. M. Biofilms: Microbial Life on Surfaces. *Emerging Infect. Dis.* **2002**, *8*, 881−890.
(39) Shina, S. Y.; Bajpaia, V. K.; Kimb, H. R.; Kanga, S. C. Antibacterial Activity of Eicosapentaenoic Acid (EPA) Against Food Borne and Dood Spoilage Microorganisms. *LWT—Food Sci. Technol.* **2007**, *40*, 1515−1519.
(40) Warnes, S. L.; Keevil, C. W. Mechanism of Copper Surface Toxicity in Vancomycin-Resistant Enterococci Following Wet or Dry Surface Contact. *Appl. Environ. Microbiol.* **2011**, *77*, 6049−6059.
(41) Sreeprasad, T. S.; Berry, V. How Do the Electrical Properties of Graphene Change with Its Functionalization? *Small* **2012**, *9*, 341−50.
(42) Biró, L. P.; Lambin, P. Grain Boundaries in Graphene Grown by Chemical Vapor Deposition. *New J. Phys.* **2013**, *15*, 035024−035062.
(43) Hod, O. Graphite and Hexagonal Boron-Nitride Have the Same Interlayer Distance. Why? *J. Chem. Theory Comput.* **2012**, *8*, 1360−1369.


DOI: 10.1021/acsami.5b01248
*ACS Appl. Mater. Interfaces* 2015, 7, 6430−6437

(44) Dean, C. R.; Young, A. F.; Meric, I.; Lee, C.; Wang, L.; Sorgenfrei, S.; Watanabe, K.; Taniguchi, T.; Kim, P.; Shepard, K. L.; Hone, J. Boron Nitride Substrates for High-Quality Graphene Electronics. *Nat. Nanotecnol.* **2010**, *5*, 722−726.
(45) Biesingera, M. C.; Laua, L. W. M.; Gersonb, A. R.; Smart, R. St.C. Resolving Surface Chemical States in XPS Analysis of First Row Transition Metals, Oxides and Hydroxides: Sc, Ti, V, Cu and Zn. *Appl. Surf. Sci.* **2010**, *257*, 887−898.
(46) Platzman, I.; Brener, R.; Haick, H.; Tannenbaum, R. Oxidation of Polycrystalline Copper Thin Films at Ambient Conditions. *J. Phys. Chem. C* **2008**, *112*, 1101−1108.



DOI: 10.1021/acsami.5b01248
*ACS Appl. Mater. Interfaces* 2015, 7, 6430−6437